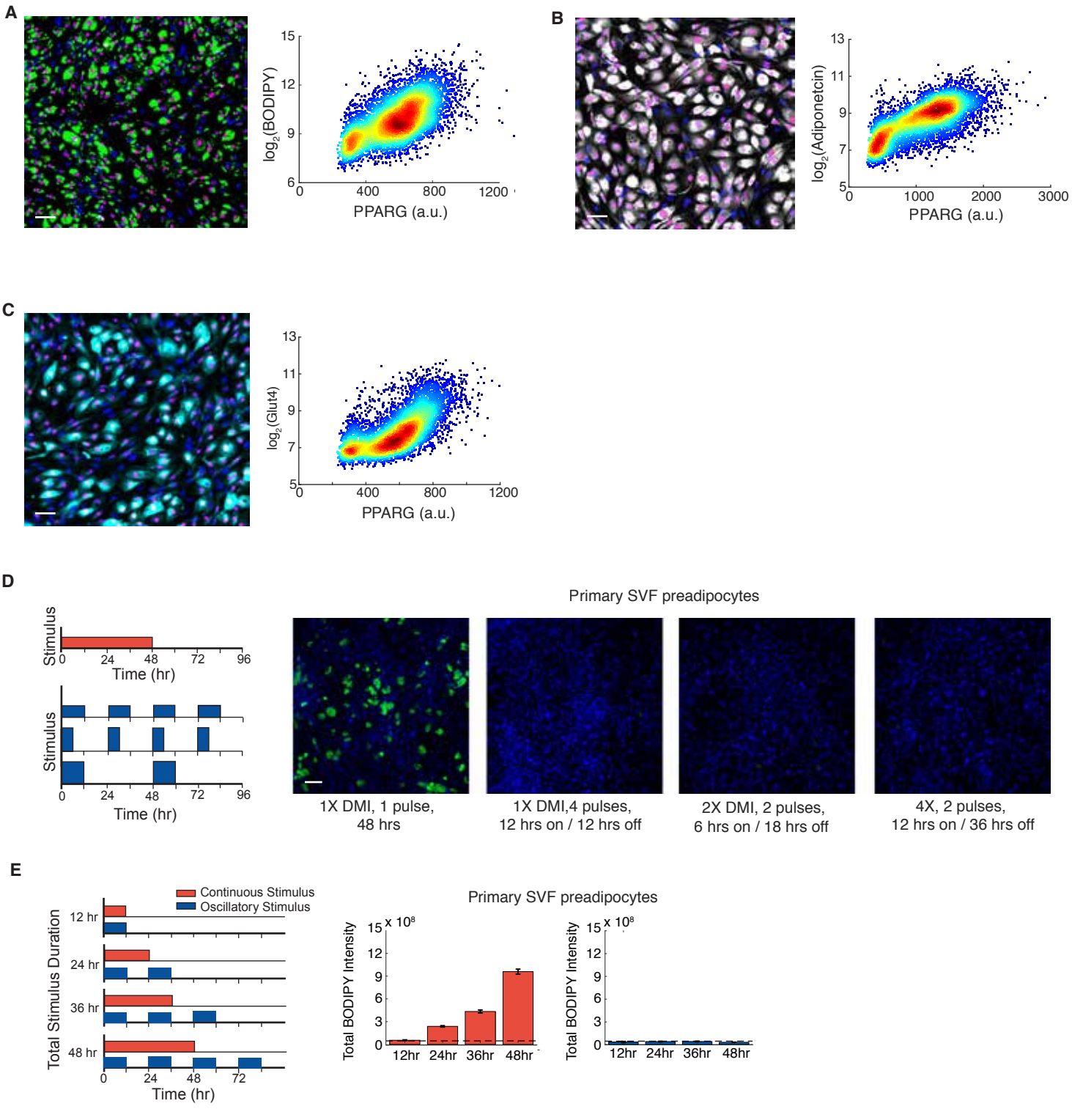


**Figure S1. Adipogenesis creates two populations of cells of low PPARG (undifferentiated) and high PPARG (differentiated cells) and the rejection of circadian hormonal pulses occurs also in primary SVF preadipocytes.**

(A-C) A 48hr DMI stimulus was applied at t=0 hrs to mouse OP9 cells. At t=96 hours, the cells were fixed and stained with Hoescht (blue) to mark nuclei and PPARG (red), plus either (A) BODIPY (green), (B) Adiponectin (white), or (C) Glut4 (blue). Images and scatter plots show that the high PPARG correlates closely with lipid accumulation (BODIPY) and markers of mature adipocytes (Adiponectin and GLUT4).

(D-E) Primary SVF preadipocytes treated with the same pulse protocols as in Figure 1D and 1E show the same rejection of circadian hormonal pulses and the same gradual increased adipogenesis for increasing continuous stimuli with durations greater than 12 hours.

(A,B,C,E) Scale bar represents 20 uM.

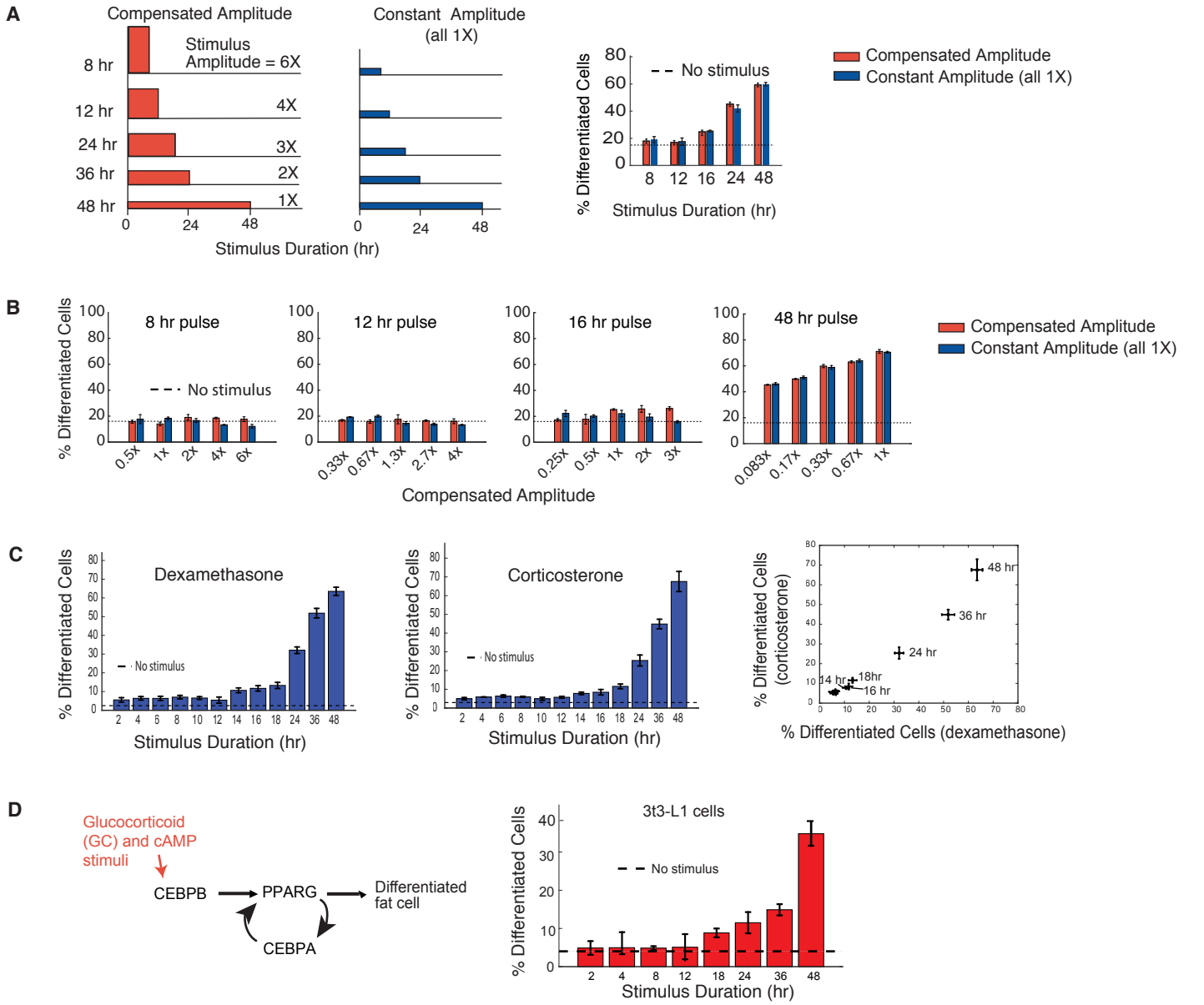


**Figure S2. Verifying that the concentration of the applied DMI pulses is not saturating and that using corticosterone, a physiological glucocorticoids, instead of dexamethasone has the same filtering effect. Also, like OP9 cells, 3T3-L1 cells filter out short and circadian glucocorticoid input signals.**

(A)Test of whether the rate of preadipocyte differentiation is controlled by the integrated strength of the stimulus or simply by the stimulus duration within a wide-range of stimulus amplitudes. (Left) Schematic showing tested protocols in which DMI stimuli was applied to OP9 preadipocyte cells for different durations at a single concentration (blue) versus at increasing concentrations that kept the total stimulus exposure constant (red). As an example of the latter, if the pulse durations were decreased by two-fold, the pulse amplitudes were increased two-fold to compensate. The cells were fixed 96 hours after application of the stimulus. (Right) Bar plots showing percent of differentiated cells for each protocol. The results show that the same rejection of differentiation stimuli less than 12 hours in duration and graded increase in differentiation rates for stimuli longer than 12 hours is seen whether or not the stimulus amplitude is increased to keep the integrated strength of the stimulus constant.

(B) Verification that the DMI stimulus concentration used is not saturating for pulsatile stimuli. The constant amplitude (1X) of the DMI stimulus was varied across a 50-fold range. Strikingly, the filtering of short duration stimuli was observed for all dilutions tested for both compensated (red bars) and constant 1X (blue bars) amplitude conditions. In contrast, increased differentiation was observed with increasing amplitudes for long 48-hour duration stimuli. (A-B)In all experiments, the 1X concentration of DMI used was 1 uM dexamethasone, 250 uM IBMX, and 1.76 nM insulin. Percent of differentiated cells, measured at 96 hours as in Figure 1B, represents mean +/- s.e.m from 3 technical replicates with approximately 7000 cells per replicate. All data shown are representative of 3 independent experiments.

(C) Using a physiological glucocorticoid, corticosterone, shows the same differentiation ability and filtering behavior as when the synthetic glucocorticoid, dexamethasone, is used. Stimuli pulses of different durations were applied to OP9 cells to indirectly activate PPARG via activation of the glucocorticoid receptor and CEBPB (DMI). For the corticosterone experiments, 1 uM corticosterone was used instead of 1uM dexamethesone in the normal DMI stimulus. The results plotted as barplots (left and middle) or in a single scatter plot (right) show that pulsing with corticosterone has the same filtering behavior as pulsing with dexamethasone. Percent of differentiated cells, quantified as in Figure 1B at 96 hours after stimuli was applied to OP9 cells to initiate adipogenesis, shows mean +/- s.e.m. from 3 technical replicates, representing 3 independent experiments.

**(D)** Bar plots showing percent of differentiated cells 96 hours after different durations of stimuli were applied to 3T3-L1 cells to initiate adipogenesis by indirectly activating PPARG via activation of the glucocorticoid receptor and CEBPB upstream of PPARG expression using DMI. Percent of differentiated cells, quantified as in Figure 1B at 96 hours after stimuli was applied to the cells to initiate adipogenesis, shows mean +/- s.e.m. from 3 technical replicates, representing 3 independent experiments.

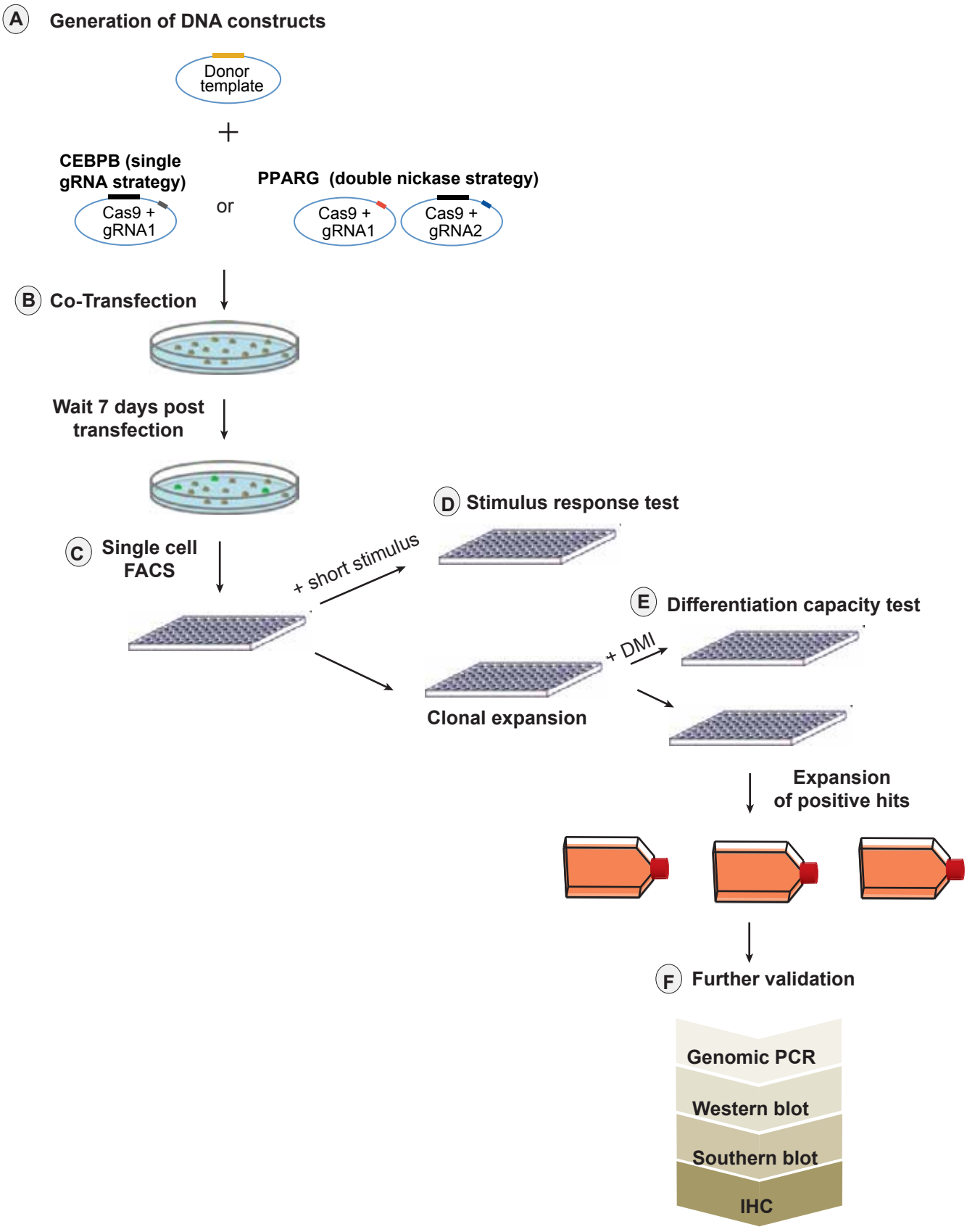


**Figure S3. Workflow for generating and validating single clones with endogenously tagged CEBPB and PPARG using CRISPR-mediated genome editing.** The different steps in the workflow are described in detail in the Methods section.

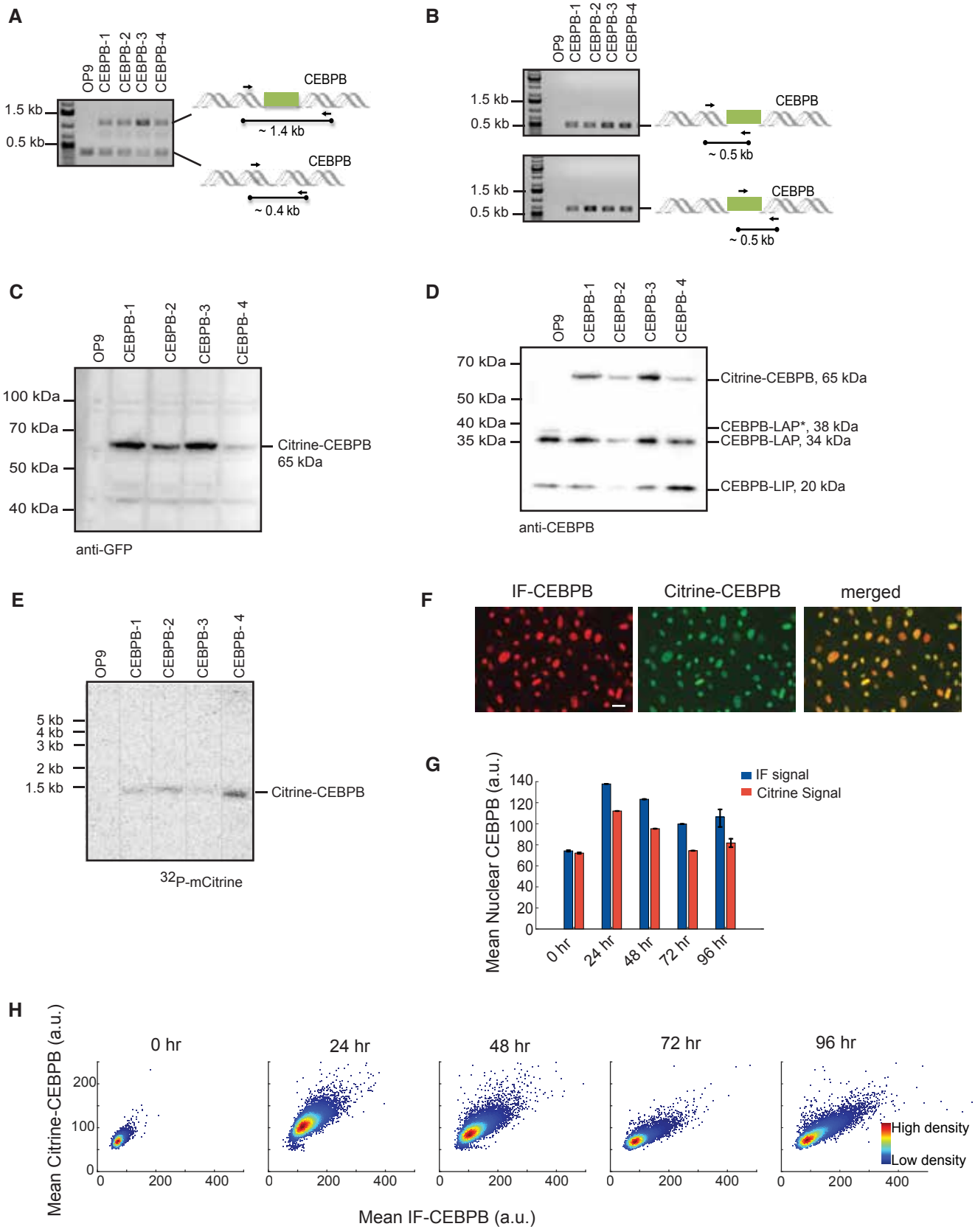


**Figure S4. Validation of CEBPB clones.** The different steps of the validation are described in detail in the Methods section.

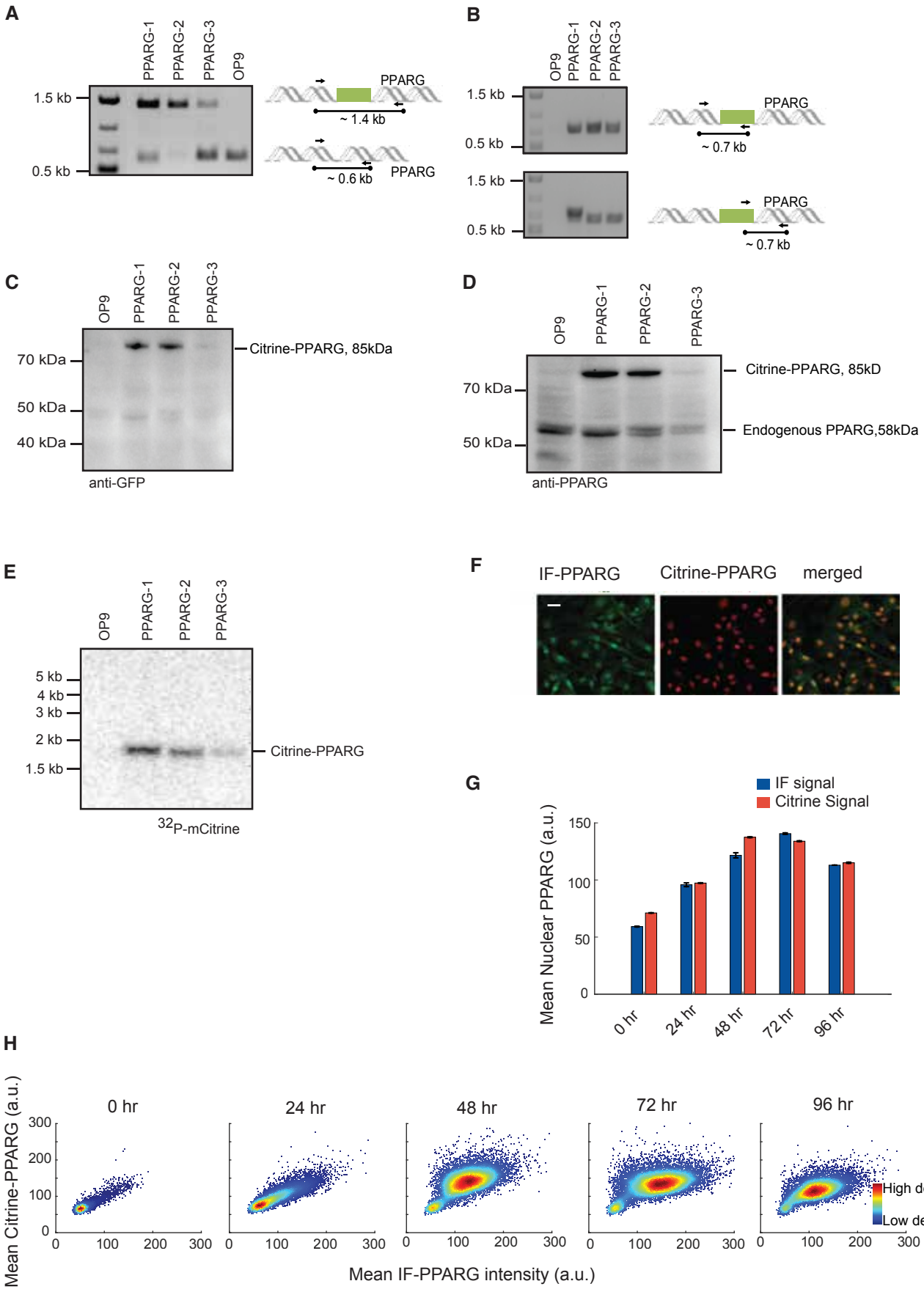


**Figure S5. Validation of PPARG clones.** The different steps of the validation are described in detail in the Materials and Methods section.

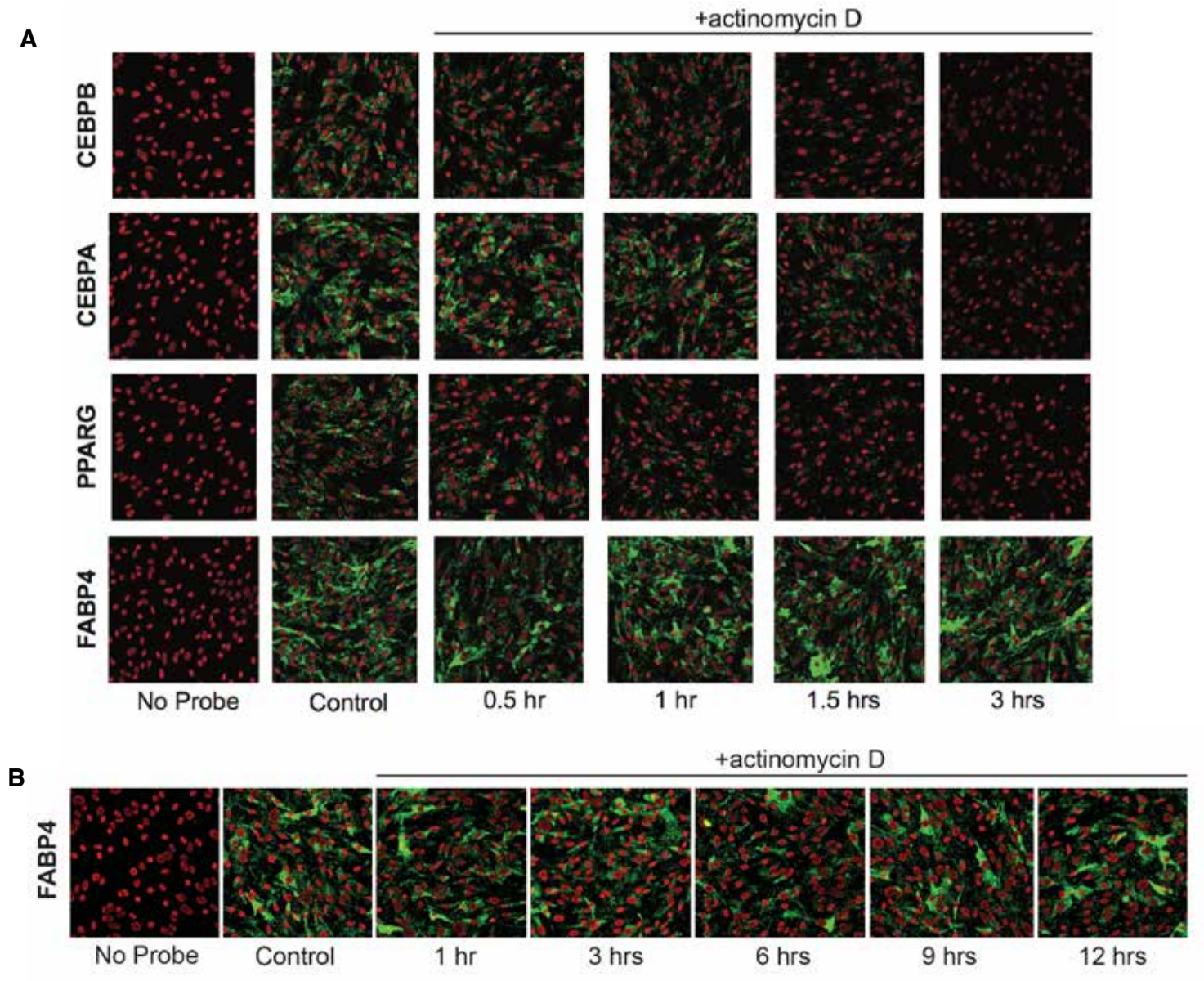


**Figure S6. Measurements of mRNA decay after addition of actinomycin D.**

(A) RNA FISH images of actinomycin D experiments. The long half-life of FABP4 mRNA is apparent by eye, even before carrying out quantitative analysis.

(B) RT-PCR measurements confirm the half-life measurements obtained by RNA FISH.

**KEY RESOURCES TABLE**

| REAGENT or RESOURCE | SOURCE | IDENTIFIER |
|---|---|---|
| **Antibodies** | | |
| Mouse monoclonal anti-PPARgamma (E-8) | Santa Cruz Biotechnology | Cat# sc-7273 |
| Rabbit polyclonal anti-PPARgamma2 | Abcam | Cat# ab45036 |
| Rabbit polyclonal anti-C/EBPβ (C-19) | Santa Cruz Biotechnology | Cat# sc-150 |
| Rabbit polyclonal anti-C/EBPα | Santa Cruz Biotechnology | Cat# sc61 |
| Rabbit polyclonal anti-FABP4 | Abcam | Cat# ab13979 |
| Rabbit polyclonal anti-GFP | Abcam | Cat# ab290 |
| Rabbit polyclonal anti-tRFP | Evrogen | Cat# EVN-AB233-C100 |
| Horseradish peroxidase (HRP)-conjugated anti-mouse | Cell Signalling | Cat# 7076 |
| horseradish peroxidase (HRP)-conjugated anti-rabbit | Cell Signalling | Cat# 7074 |
| Goat anti- Rabbit IgG (H+L) cross-adsorbed secondary antibody, alexa Fluor 514 | Invitrogen | Cat #A 31558 |
| Goat anti- Mouse IgG (H+L) cross-adsorbed secondary antibody, Alexa Fluor 594 | Invitrogen | Cat # A11032 |
| Donkey anti- Mouse IgG (H+L) cross-adsorbed secondary antibody, Alexa Fluor 647 | Invitrogen | Cat # A31571 |
| **Chemicals, Peptides, and Recombinant Proteins** | | |
| IBMX | Sigma-Aldrich | Cat # 7018 |
| Dexamethasone | Sigma-Aldrich | Cat #D1756 |
| Insulin | Sigma-Aldrich | Cat # I6634 |
| Saponin | Sigma-Aldrich | Cat #47036 |
| bovine serum albumin | Sigma-Aldrich | Cat #7906 |
| Corticosterone | Sigma-Aldrich | Cat #174 |
| Rosiglitazone | Cayman | Cat #7906 |
| BODIPY | Molecular Probes | Cat #D-3922 |
| **Experimental Models: Cell Lines** | | |
| OP9 mouse stromal | Wolins et al., 2006 | N/A |
| 3T3-L1 mouse preadipocytes cell line | Green and Kehinde, 1975 | N/A |
| **Experimental Models: Organisms/Strains** | | |
| Mouse | Jackson Labs | C57/Bl6 |
| **Oligonucleotides** | | |
| Oligonucleotide for inserting sgRNA sequences PPARG_Nterm_1_top *CACC*GAGATTTGCTGTAATTCACAC | Zhang lab web tool | N/A |
| Oligonucleotide for inserting sgRNA sequences PPARG_Nterm_1_bottom *AAAC*GTGTGAATTACAGCAAATCTC | Zhang lab web tool | N/A |
| Oligonucleotide for inserting sgRNA sequences PPARG_Nterm_2_top *CACC*GCTGTTATGGGTGAAACTCT | Zhang lab web tool | N/A |

| | | |
|---|---|---|
| Oligonucleotide for inserting sgRNA sequences PPARG_Nterm_2_bottom *AAAC*AGAGTTTCACCCATAACAGC | Zhang lab web tool | N/A |
| Oligonucleotide for inserting sgRNA sequences CEBPB_Nterm_top *CACC*GCGCGTTCATGCACCGCCTGC | Zhang lab web tool | N/A |
| Oligonucleotide for inserting sgRNA sequences CEBPB_Nterm_bottom *AAAC*GCAGGCGGTGCATGAACGCGC | Zhang lab web tool | N/A |
| Oligonucleotide for inserting sgRNA sequences FABP4_Cterm_1_top *CACCGCATAACACATTCCTAGACAC* | Zhang lab web tool | N/A |
| Oligonucleotide for inserting sgRNA sequences FABP4_Cterm_1_ bottom *AAACGTGTCTAGGAATGTGTTATGC* | Zhang lab web tool | N/A |
| Oligonucleotide for inserting sgRNA sequences FABP4_Cterm_2_top *CACCGTATGAAAGGGCATGAGCCAA* | Zhang lab web tool | N/A |
| Oligonucleotide for inserting sgRNA sequences FABP4_Cterm_1_ bottom *AAACTTGGCTCATGCCCTTTCATAC* | Zhang lab web tool | N/A |
| Primers for PPARG_Citrine_homology_donor_plasmid PPARG_homology_region1_FWD AACCAATTCAGTCGACTGGATCCAAGGCCTTAAGCAAGAAGCC | This paper | N/A |
| Primers for PPARG_Citrine_homology_donor_plasmid PPARG_homology_region1_REV ACAGCTCCTCGCCCTTGCTCACCATGGTAAGAACAGCATAAAACAGAGATTTGCTGTA | This paper | N/A |
| Primers for PPARG_Citrine_homology_donor_plasmid PPARG_homology_region2_FWD CGAGCTGTACAAGGGAGGAGGAGGTGAAACTCTGGGAGATTCTCC | This paper | N/A |
| Primers for PPARG_Citrine_homology_donor_plasmid PPARG_homology_region2_REV ATCTCGAGTGCGGCCGCGAATTCGAAATAGAGAATGCAACAT | This paper | N/A |
| Primers for PPARG_Citrine_homology_donor_plasmid PPARG_Citrine_REV TACAGCAAATCTCTGTTTTATGCTGTTCTTACCATGGTGAGCAAGGGCGAGGAGCTGT | This paper | N/A |
| Primers for CEBPB_Citrine_homology_donor_plasmid CEBPB_homology_region1_FWD AACCAATTCAGTCGACTGCGTTTGTCTCTGATGAC | This paper | N/A |
| Primers for CEBPB_Citrine_homology_donor_plasmid CEBPB _homology_region1_REV ATGGTGGCGAACGCGGGGCC | This paper | N/A |
| Primers for CEBPB_Citrine_homology_donor_plasmid CEBPB_homology_region2_FWD AGGAGGACACCGCCTGCTG | This paper | N/A |

| | | |
|---|---|---|
| Primers for CEBPB_Citrine_homology_donor_plasmid CEBPB _homology_region2_REV TCGAGTGCGGCCGCGACCTTCTTCTGC | This paper | N/A |
| Primers for CEBPB_Citrine_homology_donor_plasmid CEBPB _Citrine_FWD GCGTTCGCCACCATGGTGAGCAAGGGCGA | This paper | N/A |
| Primers for CEBPB_Citrine_homology_donor_plasmid CEBPB _Citrine_REV AGGCGGTGTCCTCCTCCCTTGTACAGCTCGTC | This paper | N/A |
| Primers for genomic PCR analysis of PPARG citrine_FWD1 CACAGAACAGTGAATGTGTGGGTC | This paper | N/A |
| Primers for genomic PCR analysis of PPARG citrine_REV2 GGAAATGGAAGCCATGAGCAG | This paper | N/A |
| Primers for genomic PCR analysis of PPARG citrine_REV3 CACAGAACAGTGAATGTGTGGGTC | This paper | N/A |
| Primers for genomic PCR analysis of PPARG citrine_FWD2 CAAGGAGGACGGCAACATC | This paper | N/A |
| Primers for genomic PCR analysis of CEBPB citrine_FWD1 CTTATAAACCTCCCGCTCGGC | This paper | N/A |
| Primers for genomic PCR analysis of CEBPB citrine_FWD1 CTTATAAACCTCCCGCTCGGC | This paper | N/A |
| Primers for genomic PCR analysis of CEBPB citrine_REV1 AAGAGGTCGGAGAGGAAGTCGT | This paper | N/A |
| Primers for genomic PCR analysis of CEBPB citrine_REV2 CTTCAGCTCGATGCGGTTCA | This paper | N/A |
| Primers for genomic PCR analysis of CEBPB citrine_FWD1 CAAGGAGGACGGCAACATC | This paper | N/A |
| **Recombinant DNA** | | |
| Plasmid: CEBPB_Citrine_homology_donor | This paper | N/A |
| Plasmid: PPARG_Citrine_homology_donor | This paper | N/A |
| Plasmid: pX330-U6-Chimeric_BB-CBh-hSpCas9 | Cong et al., 2013 | Addgene plasmid # 42230 |
| Plasmid: pX335-U6-Chimeric_BB-CBh-hSpCas9n | Cong et al., 2013 | Addgene plasmid # 42335 |
| Plasmid: mcherry | This paper | N/A |
| Plasmid: mcherry-FABP4 | This paper | N/A |
| **Other** | | |
| Zhang lab web tool for designing sgRNA | | http://crispr.mit.edu/ |
| | | |

## CONTACT FOR REAGENT AND RESOURCE SHARING

Further information and requests for reagents may be directed to, and will be fulfilled by the corresponding author, Dr. Mary N. Teruel (mteruel@stanford.edu).

## METHOD DETAILS

### Cell culture and differentiation

Primary SVF preadipocytes were cultured according to previously published protocols (Gupta et al., 2012; Ota et al., 2015) with slight modification. Briefly, stromal vascular cells (SVC) were isolated from inguinal subcutaneous WAT from 6-8 week old male C57BL/6J mice. The tissue was rinsed in PBS, minced, and digested with 1mg/ml collagenase type D (Roche 11088866001) and 1mg/ml Dispase II (Sigma-Aldrich D4693) in PBS with 1mM $CaCl_2$ for 40 minutes in a 37C shaking water bath. The digest was filtered to exclude large debris and separated into the adipocyte (supernatant) and SVC fractions (pellet) by spinning cells at 300 RCF for 3 minutes. The SVC fraction, which contains preadipocytes, was washed once and then plated in warm culture medium (DMEM with 10% FBS + 100U/mL pen/strep + 2.5ug/ml amphotericin B) for 2 hours and then washed with culture media to remove cell debris and non-adherent cells, thus enriching for preadipocytes which adhere well to the culture surface. Cells were further grown in culture for one to two passages before plating cells for experiments.

OP9 and 3T3-L1 cells were cultured according to previously published protocols (Ahrends et al., 2014; Park et al., 2012; Wolins et al., 2006). OP9 cells were cultured in growth media consisting of MEM-α (Invitrogen, # 12561) and 100 units/mL Penicillin, 100$\mu$g/mL Streptomycin, and 292 µg/mL L-glutamate (Invitrogen, # 10378-016), plus 20% Fetal Bovine Serum (FBS). 3T3-L1 cells were cultured in growth media consisting of DMEM, 2 mM l-glutamine, 100 U/ml penicillin, and 100 U/ml streptomycin, plus 10% bovine calf serum.

To induce differentiation of SVF preadipocytes, OP9 cells, and 3T3-L1 cells, confluent cells were treated with a differentiation medium containing a commonly used DMI (dexamethasone /

IBMX / insulin) stimulus to initiate adipogenesis. DMI consists of dexamethasone (dex), a synthetic glucocorticoid; 3-isobutyl-1-methylxanthine (IBMX), an inhibitor of phosphodiesterase that increases cAMP levels; and insulin. Applying the DMI stimulus consisted of replacing the media on the cells with growth media plus 10% FBS, 0.25 mM IBMX (Sigma Cat # 7018), and 1 uM dexamethasone (Sigma Cat #D1756) (Stimulus I). Two days after initiating differentiation, Stimulus I was removed from the cells and was replaced with Stimulus II consisting of growth media plus 10% FBS and 1.75 nM insulin (Sigma Cat # I6634) for two more days. As noted in some experiments, corticosterone (Sigma Cat #174) was used instead of dexamethasone. Also, for other experiments as noted, rosiglitazone (Cayman, USA) was added to the media to result in a final concentration of 1 to 10 uM.

To apply pulses of dexamethasone, corticosterone, or other stimuli, the current media on the cells was gently removed. To remove all traces of the previous stimulus, the cells were then washed by adding fresh growth media to the cells and removing it three times. Then the new stimulus was applied to the washed cells.

**Immunofluorescence Staining**

OP9, 3T3-L1, and SVF preadipocyte cells were fixed with 3% paraformaldehyde in PBS for 30 min. Then the cells were gently washed 3X with PBS. Permeabilization was carried out with 0.1 % Triton X-100 in PBS for 15 minutes on ice, followed by blocking with 5% bovine serum albumin (Sigma #7906). The cells were stained with DAPI (1:20000), anti-PPARG (1:1000 Santa Cruz Biotech #sc-7273), anti-PPARG2 (Abcam ab45036), anti-CEBPB (1:1000, Santa Cruz Biotech #sc-150), anti-CEBPA (1:1000, Santa Cruz Biotech #sc61), or anti-FABP4 (1:200, Abcam, #ab13979). Alexa Fluor-514 (#A31558), 594 (#A11032) and 647 (#A31571) (1:1000, Invitrogen) were used as secondary antibodies.

In cases in which BODIPY was used to stain lipids, permeablization was carried out more gently using 0.05% saponin (Sigma #47036), to better preserve the lipid structure, followed by

blocking with 5% bovine serum albumin (Sigma #7906). The cells were then stained with the antibodies listed above, plus BODIPY 493/503 (1$\mu$g/ml, Molecular Probes #D-3922).

**Defining differentiation**

We have previously shown that the transition from a proliferating preadipocyte precursor cell into a mature, non-proliferating adipocyte capable of accumulating lipid occurs via a bistable switch from low PPARG expression in the cell to high PPARG expression (Ahrends et al., 2014; Park et al., 2012). As shown in Figure 1B, a histogram of PPARG expression for a population of differentiating adipocytes shows two peaks of PPARG expression - low and high. The high state predicts the subsequent lipid droplet formation. We thus define a cell as being differentiated if its level of PPARG placed the cell in the high PPARG-expressing peak of the cell population which correlates with high lipid accumulation and markers of mature adipocytes such as adiponectin and GLUT4 (Figures 1B, S1A, and S1B).

**siRNA preparation and transfection**

Diced pool siRNA for CEBPB and YFP was generated as described previously (2, 3). OP9 cells were transfected with siRNA by a reverse transfection protocol. For each 96-well well, 2 pmol of diced-pool siRNA were diluted in 10$\mu$l of Opti-Mem I Medium. 0.2$\mu$l of RNAiMax (Invitrogen #13778150) diluted in 10$\mu$l of Opti-Mem I was then added, mixed well, and then incubated for 10 minutes at room temperature. This mixture was then placed into a 96-well, and OP9 cells were added (15,000 cells suspended in 80 $\mu$l of growth medium without antibiotics). After 24 hours, the media was replaced with differentiation media to induce differentiation following differentiation method. siRNA for FABP4 (Dharmacon ON-TARGETplus SMARTpool #11770) and AllStars Negative Control siRNA (Qiagen #SI03650318) were purchased from the respective manufacturers and were transfected using lipofectamine RNAiMax (Invitrogen #13778150), following manufacture suggested protocol for forward SiRNA transfection.

**Measuring protein decay rates using cyclohexamide**

To obtain protein decay rates, 10,000 OP9 cells were seeded in 96-well plates) one plate for each timepoint. Cells were induced to differentiatiate with DMI for 24 hours. Cyclohexamide was added at a final concentration of 30uM. Cells were fixed and stained at different times after addition of cyclohexamide, and immunofluorescence was used to quantify protein concentration following the protocol shown in Figure 1B. Half-lives were obtained by fitting first order exponential decay curves to the data.

**Measuring mRNA decay rates using Actinomycin D and RNA FISH**

To carry out an mRNA decay timecourse, 10,000 OP9 cells were seeded in 96-well glass plates (Greiner), one plate for each timepoint. Actinomycin D (Cat #A1410, Sigma) was applied 5 minutes before the first timepoint (t=0 hours) at a concentration of 5ug/ml. Cells were fixed with 4% formaldehyde for 15 min, stored in 75% ethanol at 4°C. RNA FISH was performed using the Affymetrix Quantigene ViewRNA ISH cell assay (Affymetrix eBioscience, San Diego, CA). FISH probes for mouse PPARG, CEBPA, CEBPB, and FABP4 were purchased from Affymetrix eBioscience. Cells were rehydrated in PBS for 10 minutes and then permeabilized with a detergent solution provided by the assay kit for 5 min at room temperature. The cells were incubated with diluted FISH probes (1:25) at 40°C for 3 hrs. Cells were then hybridized with the three different probes provided by the assay kit: preamplification probe, amplification probe, and label probe which were carried out by incubating cells with a probe for 30 min at 40°C. Finally, cells were incubated with Hoechst (1:10,000 in PBS) for 5 min, washed three times with PBS, and left in PBS for imaging.

**Image Acquisition**

Images were acquired on an ImageXpress MicroXL automated epifluorescence microscope (Molecular Devices; Sunnyvale, CA, USA) using 10X Plan Fluor objective and a 2560 x 2160 pixel

Andor Zyla 5.5 sCMOS camera with a 16-bit readout. A camera bin of 1 was used for fixed cell imaging, and a camera bin of 2 was used for live cell imaging.

For fixed-cell imaging, cells were plated in 96-well, optically clear, polystyrene plates (Costar #3904) For live-cell imaging, 7,000 - 8,000 OP9 cells were plated >6-12 hours prior to imaging in full growth media in 96-well optically clear, glass-bottom plates (either Greiner Sensoplate or Invitro Scientific).

Living cells were imaged in FluoroBrite DMEM media (Invitrogen) to reduce background fluorescence. Before image acquisition, the full growth media was switched to media consisting of FluoroBrite DMEM with 10% FBS and 1% Penicillin/Streptomycin. Time-lapse imaging was performed in 200 ul of media per well. Cells were imaged in a humidified 37degC chamber at 5% $CO_2$. Images were taken every 10 min in CFP, YFP, RFP channels (depending on the experiment). Total light exposure time was kept less than 600 ms for each time point. Two, non-overlapping sites were imaged per well.

**Image Processing and Analysis**

Segmentation

Cells were segmented for their nuclei based on either Hoechst staining (fixed-cell imaging) or H2B-Turquoise (live-cell imaging). Nuclear segmentation was performed as follows: A Laplacian of Gaussian filter was applied to the nuclear image to identify the edges of cell nuclei. Pixels within the nuclei edges were identified as cell nuclei and pixels outside the nuclei edges were identified as background. To split cells in contact with their nearest neighbor(s), a custom segmentation algorithm was implemented to detect and bridge concave inflections in the perimeter of each object (hereafter referred to as the 'deflection bridging algorithm').

Signal Measurement

Each channel global background subtraction was used to measure all immunofluorescence and fluorescent protein intensities as follows: the nuclear mask was dilated by 50 μm and the background

for the image was calculated as the mode pixel intensity of all non-masked pixels. Nuclear immunofluorescence and nuclear fluorescent protein signals were calculated as median nuclear intensity. In the case of CEBPB, the sum nuclear intensity was used instead because it exhibited a punctate pattern due to its centromeric localization in the nucleus.

Tracking

The deflection-bridging algorithm was implemented on every object in the first imaging frame, and then only adaptively in subsequent frames. This was accomplished by iteratively tracking cells in each frame, detecting probable merge events (as discussed below), and selectively implementing the deflection-bridging algorithm on putative merged objects. This method reduced the probability of over-segmentation, increased processing speed, and improved tracking fidelity. Tracking of cells between frames was implemented by screening the nearest future neighbor for consistency in total H2B-Turquoise fluorescence. This 'conservation of total fluorescence' was further exploited to detect merges or splits, which allowed recovery of overlapping traces. Mitosis events (called at anaphase) were called when the total H2B fluorescence of the two nearest future neighbors of a given cell were both between 45-55% of the total H2B fluorescence of the past cell. Frame-to-frame jitters were accounted for by registering sequential H2B-Turquoise images by cross-correlation.

**Workflow used to generate single OP9 cell colonies with endogenously tagged CEBPB and PPARG (Figure S3):**

A) Construction of DNA plasmids

A.1) Construction and design of the donor template

CRISPR-mediated genome editing was used to tag the N-terminus of endogenous PPARG and CEBPB with Citrine (Griesbeck et al., 2001), a bright version of the yellow fluorescent protein. We tagged the PPARG2 isoform since it is the PPARG isoform that is highly expressed in adipose tissue and that controls fat cell differentiation. CEBPB has three isoforms LAP*, LAP, and LIP, and we chose to tag the longest isoform LAP* at the N-terminus. The DNA repair template to promote homology directed repair (HDR)-mediated insertion of the fluorescent protein (FP) was constructed by inserting the cDNA of FP-3xGly flanked by two 800 bp homology arms into the entry vector backbone pENTR1a (Addgene Plasmid #17398). The repair template was assembled such that after HDR, the FP is inserted in frame at the N-terminus and separated with a 3xGly linker from PPARG and CEBPB, respectively. The pENTR1a backbone vector was digested with *EcoR*I-HF and *BamH*I-HF (NEB), and assembled together with three DNA fragments coding for homology arm 1, Citrine or mKate2, and homology arm 2 using Gibson assembly(Gibson et al., 2009). The homology arm fragments were PCR amplified from OP9 genomic DNA with primers introducing a 15-20 bp overhang used for Gibson assembly. Similarly, the FP was PCR amplified from a DNA template using primers introducing the linker and an overhang for Gibson assembly. The sequences of the assembled donor vector constructs were verified by sequencing.

A.2) Construction of the Cas9 plasmids

To carry out CRISPR genome editing to make Citrine-CEBPB, we used Plasmid pX330-U6-Chimeric_BB-CBh-hSpCas9 (pX330) (Addgene plasmid # 42230) to deliver the SpCas9 protein and guide RNA (Cong et al., 2013). A 20 nucleotide “targeting” sequence was inserted into the guide sequence insertion site of the pX330 plasmid to produce guide RNAs directed to the N-terminal of

CEBPB. Targeting sequences were designed using the web tool, crispr.mit.edu. From the predicted target sites, the sequences with the highest scores and in proximity of the ATG were selected. To carry out CRISPR genome editing to make Citrine-PPARG, we initially used the same single guide RNA strategy to insert citrine at the N-terminus of PPARG. However, we found that the majority of PPARG clones generated using SpCas9 had undesired off-target integrations of Citrine into the OP9 genome. To reduce off-target integration events we switched to using the "double nickase" system which uses two different guide RNAs that create adjacent and opposing nicks in the DNA at the site of insertion (Ran et al., 2013). We found that using the double-nickase system greatly improved the specificity of Cas9-mediated double strand breaks at the PPARG locus. To carry out double-nickase genome-editing, two different targeting sequences directed to the PPARG locus were designed as described above and inserted into the guide RNA site of two plasmids, pX335-U6-Chimeric_BB-CBh-hSpCas9n (pX335) (Addgene plasmid # 42335) encoding the SpCas9 D10A nickase. Oligonucleotide duplexes encoding each desired targeting sequence were ligated into the *Bbs*I cut sites of px330 or px335 , respectively. All constructs were validated by sequencing.

B) Transfection

To endogenously tag PPARG with Citrine, 1 µg of each of the two pX335 guide RNA/SpCas9n constructs and 5 µg of the Citrine donor template were transfected into 1 million OP9 cells using Lipofectamine 2000 (Invitrogen) following the manufacturer's protocol. To endogenously tag CEBPB with Citrine, 2 µg of the desired pX330 guide RNA/SpCas9 construct and 5 µg the Citrine donor template were transfected into 1 million OP9 cells using Lipofectamine 2000.

C) Clone selection by single-cell FACS

Seven days post-transfection, single cells expressing Citrine were sorted into separate wells of 96-well culture plates and allowed to grow. We chose to wait 7 days post transfection to avoid false positive fluorescent signal originating from the un-integrated donor DNA plasmid.

D) Stimulus Response Test

Once the single-cell colonies grew to 50% confluency, each colony was passaged into wells on two different 96-well plates. One plate was used to expand the colonies, and the other half was imaged using a Molecular Devices MicroXL fluorescence imaging system to select for clones with correct localization of the Citrine signal and the appropriate response to stimuli. Before imaging, PPARG clones were stimulated with Rosiglitazone for 24 hours to induce expression of the Citrine-PPARG, and CEBPB clones were stimulated for 24 hours with DMI to induce expression of Citrine-CEBPB.

E) Differentiation capacity test

Clones that expressed Citrine were further characterized for their differentiation capacity using the standard four-day adipocyte differentiation protocol detailed under “Cell Culture and Differentiation.” Clones that acquired mature adipocyte morphology and accumulated lipid droplets in response to DMI treatment were expanded and subjected to further validation steps.

F) Further validation

F.1) Validation of citrine-CEBPB clones

We first performed genomic PCR with different primer sets to look at the genotype and verify correct insertion of Citrine into the CEBPB locus. The first PCR was performed using primers annealing to regions flanking the site where Citrine is inserted (Supp. Table 3, Figure S5A). Using this set of primers, CEBPB tagged clones were shown to be heterozygous, and the PCR products were subjected to sequencing. The second set of PCRs was performed using primers annealing to regions around 5’ and 3’ ends of the inserted Citrine. (Supp. Table 4, Figure S5B). Both reactions resulted in a single band, indicating that Citrine was correctly inserted into the 5’ end of the CEBPB locus in all clones.

Next, Western blot analysis of citrine-CEBPB clones was performed using anti-GFP antibody and anti-CEBPB to verify protein expression and to check for the correct molecular weight of the tagged protein (Figures S5C-D). The size compatible with the correct predicted molecular weight of citrine-protein fusion were shown for each clone. The anti GFP blot shows the expression of tagged-CEBPB and did not detect any free GFP. The anti CEBPB blot shows the expression of the three CEBPB isoforms (LAP*, LAP, LIP) in OP9 cells. In the citrine-CEBPB clones, the LAP* isoform is shown to be tagged with citrine as expected.

Next, Southern blot analysis was performed to confirm locus-specific knock-in using a probe directed towards citrine. All examined clones showed the presence of a specific copy of citrine within the genome, as evidenced by the detection of a single band of expected size (1.5kb) in the Southern blot (Figure S5E).

Finally, immunohistochemistry analysis was used to validate correct nuclear localization and differentiation capacity of the clones (Figure S5F-H). Colocalization of the citrine fluorescence signal with the immunohistochemistry signal of the untagged proteins throughout four days of differentiation, was used to choose clones for live cell imaging. The selected clone CEBPB-3 differentiated well and showed similar expression of citrine-CEBPB and untagged CEBPB over the timecourse of differentiation (Figure S5F). Thus, clone CEBPB-3 was subsequently used for all further experiments.

F.2) Validation of citrine-PPARG clones

The same steps used for CEBPB validation were used to validate the PPARG clones (Figure S4). Since it passed all the validation criteria described above, the PPARG-2 clone was used for all the timecourse measurements in the current manuscript.

**T7 assay**

The cutting efficiency of Cas9 with the designed guide RNAs was determined using a T7

Endonuclease assay. The assembled plasmids (pX330 or pX335) were transfected together into OP9 cells with a construct containing mCherry in the Clontech C1-vector (mcherry-C1). The mCherry-C1 served as a co-transfection marker for cells that are likely transfected with pX330 or pX335 plasmids. The constructs were transfected at a 1:10 ratio of gRNA-pX330 or gRNA-pX335 to mCherry-C1 into OP9 cells using Lipofectamine 2000 (Invitrogen) following the manufacturer's protocol. Seventy-two hours post-transfection, the mCherry-C1 expressing cells were sorted by FACS, grown up using our standard cell culture protocol, and genomic DNA was extracted using a Qiagen DNeasy Blood and Tissue kit. Approximately 600 bp of the genomic DNA (~200 and 400 bp around the predicted cut site) was amplified by PCR and used for a T7 assay that was carried out using Surveyer® mutation kit hybridization conditions (IDT, cat # 706020). Briefly, 200ng DNA was hybridized in a thermocycler to form heteroduplexes of cut and uncut DNA strands, incubated with T7 endonuclease I (New England Biolabs, Cat #M0302S) for 1 hour at 37 °C to cleave mismatched heteroduplexes, run on a 10% TBE polyacrylamide gel (Invitrogen) and stained with ethidium bromide. The fraction of strands that were cleaved by T7 endonuclease, as visualized by the gel, is representative of the cutting efficiency of the CRISPR constructs. For each site of interest, the CRISPR construct that showed the highest cutting efficiency was used to direct insertion of Citrine.

**Western Blot Analysis**

CRISPR-tagged clones and wtOP9 cells were stimulated for 48h with Rosiglitazone (Citrine-PPARG and FABP4-mKate2 clones) or for 12h with DMI (Citrine-CEBPB clones) to increase protein levels for western blot analysis of PPARG and CEBPB, respectively. The presence and integrity of Citrine-tagged proteins was verified with an antibody directed to the tagged protein and by immunoblotting for GFP. Cell pellets of citrine-PPARG clones were lysed on ice with nuclear extraction kit (Abcam), according to the manufacturer's protocol, and quantified using a BCA assay (Thermo Scientific). For citrine-CEBPB clones, cells were lysed on ice in RIPA lysis buffer (Millipore, CA) in the presence of protease inhibitors (cOmplete™, Mini, EDTA-free, Sigma Aldrich). All samples were boiled for 10 min

at 96 °C in NuPAGE LDS sample buffer containing 1x reducing agent (Invitrogen). Lysates were separated by SDS–PAGE using the XCell SureLock Electrophoresis Cell on NuPAGE™ Novex™ 4-12% Bis-Tris Protein Gels (Invitrogen). Proteins were transferred onto polyvinylidene fluoride membranes (Thermo Scientific) using the XCell II Blot Module (Invitrogen). Membranes were blocked by incubating with TBS with 0.1% Tween-20 containing 5% non-fat milk for 2h at room temperature or overnight at 4 °C for anti-GFP. Membranes were subsequently incubated overnight at 4 °C with primary antibodies at a dilution of 1:1,000 (anti-PPARG, Santa Cruz Biotech #sc-7273) and 1:2,000 (anti-CEBPB antibody, Santa Cruz Biotech #sc-7962) in blocking buffer or for 1h at RT at a dilution of 1:2,500 (anti-GFP abcam #ab290). Membranes were washed 3 times for 5 min using wash buffer (TBS with 0.1% Tween-20), and further incubated in 1:5,000 horseradish peroxidase (HRP)-conjugated secondary antibodies (anti-mouse and anti-rabbit (Cell Signalling #7076 and #7074) for 1 h at room temperature. After another set of three washes, antibody-bound proteins were visualized on film using supersignal™ West Femto chemiluminescence substrate (Thermo Scientific).

**Southern blot analysis**

To check whether Citrine and mKate2 was integrated at any unspecific loci, a southern blot was performed with a $^{32}$P-labeled probe directed towards Citrine. Two probes about 500 bp was amplified by standard PCR from a Citrine plasmid and gel purified. The labeled probe was prepared with the RadPrime DNA kit (Invitrogen) in the presence of dCTP [α-$^{32}$P] (Perkin Elmer) and a clean-up step was performed using illustra™ Microspin™ G-25 Columns (GE Healthcare), all according to the manufacturer's guidelines. Genomic DNA was extracted using a Qiagen DNeasy Blood and Tissue kit, and 7 µg DNA was digested overnight. Digestion enzymes were chosen such that they cut around Citrine and generate fragments of ~1.8 kb, ~1.5kb and 1.9 kb for PPARG and CEBPB, respectively. Digested samples were separated with 1% agarose gel electrophoresis, and the gel was incubated 1x 20-min in 0.25M HCl followed by 2x 15-min in 0.5M NaOH/1.5M NaCl to denature

the dsDNA. Subsequently, 2x 15-min washes were performed in transfer buffer (1M $NH_4OAc$) to neutralize the gel. The DNA fragments were transferred via capillary forces from the gel to an Amersham Hybond-N+ membrane (GE Healthcare). Afterwards, the DNA was cross-linked to the membrane using ultraviolet light (0.3J/$cm_2$; UVStratalinker 1800, Stratagene, La Jolla, CA). After 1h of prehybridization of the membrane at 65 °C in a Techne hybridizer HB-1D in hybridization buffer (0.5M sodium phosphate buffer pH 7.2, 7% SDS), the probe was hybridized overnight at 65 °C in the presence of salmon sperm DNA (100 µg/ml) to avoid unspecific binding of the probe. After hybridization, the blots were washed at hybridization temperature for 2x 15-min in each of the following buffers in sequential order: 0.3x SSC, 0.1% SDS, 0.1x SSC, 0.1% SDS 0.1x SSC, 1.5% SDS. The probe was visualized using a storage phosphor screen and Typhoon™ imager (GE Healthcare).

**Description of Model**

$$\frac{dPPARG}{dt} = b_{PPARG} + \frac{2*(Stim+CEBPA)^4}{3+(Stim+CEBPA)^4} - k_{deg\_PPARG} * PPARG$$

$$Z = PPARG * \left(0.2 + \frac{FABP4}{1+FABP4}\right)$$

$$\frac{dCEBPA}{dt} = noise * \left[b_{CEBPA} + \left(\frac{2*Z^2}{1+Z^2}\right)\right] - k_{deg\_CEBPA} * CEBPA$$

$$\frac{dFABP4}{dt} = b_{FABP4} + \left(\frac{0.1*Z^2}{0.5+Z^2}\right) - k_{deg\_FABP4} * FABP4$$

$$b_{PPARG} = 0.03$$
$$b_{CEBPA} = 0.02$$
$$b_{FABP4} = 0.003$$
$$k_{deg\_PPARG} = 0.6931$$
$$k_{deg\_CEBPA} = 0.1980$$
$$k_{deg\_FABP4} = 0.023$$

1) *Stim* represent the stimulus. Assume *Stim* ~ CEBPB
2) In the first equation, *Stim* and CEBPA are added together because CEBPB and CEBPA bind to the same DNA sequences and can replace each other at binding sites.
3) Cooperativity of 4 for (*Stim*+CEBPA) because CEBPB and CEBPA have to dimerize in order to function and there are multiple CEBPB/CEBPA binding sites on the PPARG promoter.
4) Z represents that FABP4 needs to activate PPARG in order for PPARG to have transcriptional activity on target genes like FABP4 and CEBPA.
5) FABP4's activation of PPARG is limited such that it can only increase 6-fold (max. Z = 1.2 * PPARG).
6) Cooperativity of 2 in the second and third equations because there are multiple binding sites for PPARG on the CEBPA and FABP4 promoters
7) Degradation rates correspond to 1 hour for PPARG, 3.5 hours for CEBPA, and 30 hours for FABP4.
8) Lognormal noise (with mean=0, standard dev=30%) randomly to each simulation shown in Figures 7G and 7H through a noise term before the PPARG term in the equation calculating dCEBPA/dt. A noise term was added only to one equation for simplicity. We have established in previous work that adding a larger noise to a single parameter is similar to adding smaller noise terms to each parameter in different equations (Ahrends et al., 2014).

| **Target** | **Strand** | **Oligonucleotide sequence (5′ to 3′)** |
|---|---|---|
| PPARG_Nterm_1 | Top | *CACC*GAGATTTGCTGTAATTCACAC |
| PPARG_Nterm_1 | Bottom | *AAAC*GTGTGAATTACAGCAAATCTC |
| PPARG_Nterm_2 | Top | *CACC*GCTGTTATGGGTGAAACTCT |
| PPARG_Nterm_2 | Bottom | *AAAC*AGAGTTTCACCCATAACAGC |
| CEBPB_Nterm | Top | *CACC*GCGCGTTCATGCACCGCCTGC |
| CEBPB_Nterm | Bottom | *AAAC*GCAGGCGGTGCATGAACGCGC |

**Table S1: Oligonucleotide sequences used to insert sgRNA sequences into the px335 or px330 expression vector.** Guide sequences are targeted to the PPARG and CEBPB N-terminal. The underlined and italicized nucleotides denote the overhang for ligation of the oligonucleotide duplex into the px335 or px330 guide sequence insertion site.

| Primer Name | Template | Primer sequence (5′ to 3′) |
|---|---|---|
| PPARG_homology_region1_FWD | OP9 genomic DNA | AACCAATTCAGTCGACTGGATCCA AGGCCTTAAGCAAGAAGCC |
| PPARG_homology_region1_REV | OP9 genomic DNA | ACAGCTCCTCGCCCTTGCTCACCA TGGTAAGAACAGCATAAAACAGAG ATTTGCTGTA |
| PPARG_homology_region2_FWD | OP9 genomic DNA | CGAGCTGTACAAGGGAGGAGGAG GTGAAACTCTGGGAGATTCTCC |
| PPARG_homology_region2_REV | OP9 genomic DNA | ATCTCGAGTGCGGCCGCGAATTC GAAATAGAGAATGCAACAT |
| PPARG_Citrine_FWD | Citrine plasmid | TACAGCAAATCTCTGTTTTATGCTG TTCTTACCATGGTGAGCAAGGGCG AGGAGCTGT |
| PPARG_Citrine_REV | Citrine plasmid | CTTGTACAGCTCGTCCATGCCGA |
| CEBPB_homology_region1_FWD | OP9 genomic DNA | AACCAATTCAGTCGACTGCGTTTG TCTCTGATGAC |
| CEBPB _homology_region1_REV | OP9 genomic DNA | ATGGTGGCGAACGCGGGGCC |
| CEBPB_homology_region2_FWD | OP9 genomic DNA | AGGAGGACACCGCCTGCTG |
| CEBPB _homology_region2_REV | OP9 genomic DNA | TCGAGTGCGGCCGCGACCTTCTTC TGC |
| CEBPB _Citrine_FWD | Citrine plasmid | CGCGTTCGCCACCATGGTGAGCA AGGGCGA |
| CEBPB _Citrine_REV | Citrine plasmid | AGGCGGTGTCCTCCTCCCTTGTAC AGCTCGTC |

**Table S2: Primers used for PCR amplification of fragments that were joined by Gibson assembly to create donor vectors to insert Citrine at the N-terminals of PPARG and CEBPB via homologous recombination.**

| **Assay** | **Primer sequence (5′ to 3′)** | **Amplicon (bp)** |
|---|---|---|
| genotyping PPARG Citrine clones | **FWD:** CAC AGA ACA GTG AAT GTG TGG GTC | **630** (wt allele) **1347** (knock-in allele) |
| | **REV:** GGA AAT GGA AGC CAT GAG CAG | |
| genotyping CEBPB Citrine clones | **FWD:** CTT ATA AAC CTC CCG CTC GGC | **360** (wt allele) **1077** (knock-in allele) |
| | **REV:** AAG AGG TCG GAG AGG AAG TCG T | |

**Table S3: Primers used for genomic PCR analysis of the PPARG and CEBPB CRISPR clones.**

| **Assay** | **Primer sequence (5′ to 3′)** | **Amplicon (bp)** |
|---|---|---|
| seq. 1<br>PPARG Citrine clones | **FWD:** CAC AGA ACA GTG AAT GTG TGG GTC | - (wt allele)<br>**717** (knock-in allele) |
| | **REV:** CTT CAG CTC GAT GCG GTT CA | |
| seq. 2<br>PPARG Citrine clones | **FWD:** CAA GGA GGA CGG CAA CAT C | - (wt allele)<br>**650** (knock-in allele) |
| | **REV:** GGA AAT GGA AGC CAT GAG CAG | |
| seq. 1<br>CEBPB Citrine clones | **FWD:** CTT ATA AAC CTC CCG CTC GGC | - (wt allele))<br>**475** (knock-in allele) |
| | **REV:** CTT CAG CTC GAT GCG GTT CA | |
| seq. 2<br>CEBPB Citrine clones | **FWD:** CAA GGA GGA CGG CAA CAT C | - (wt allele)<br>**603** (knock-in allele) |
| | **REV:** AAG AGG TCG GAG AGG AAG TCG T | |

**Table S4: Primers used for genomic PCR analysis to verify the fluorophore integration sites of the PPARG and CEBPB tagged clones.**

| **Primer Name** | **Primer sequence (5′ to 3′)** |
|---|---|
| Citrine_probe_FWD | CGACGTAAACGGCCACAAGTT |
| Citrine_probe_REV | ATGGGGGTGTTCTGCTGGTAGT |

**Table S5: Primers used for the PCR amplification of a 504 bp probe directed towards Citrine.**

**REFERENCES**


Ahrends, R., Ota, A., Kovary, K.M., Kudo, T., Park, B.O., and Teruel, M.N. (2014). Controlling low rates of cell differentiation through noise and ultrahigh feedback. Science *344*, 1384–1389.

Cong, L., Ran, F.A., Cox, D., Lin, S., Barretto, R., Habib, N., Hsu, P.D., Wu, X., Jiang, W., Marraffini, L., et al. (2013). Multiplex Genome Engineering Using CRISPR/Cas Systems. Science *339*, 819–823.

Gibson, D.G., Young, L., Chuang, R., Venter, J.C., Hutchison, C. a, and Smith, H.O. (2009). Enzymatic assembly of DNA molecules up to several hundred kilobases. Nat. Methods *6*, 343–345.

Griesbeck, O., Baird, G.S., Campbell, R.E., Zacharias, D.A., and Tsien, R.Y. (2001). Reducing the environmental sensitivity of yellow fluorescent protein. Mechanism and applications. J. Biol. Chem. *276*, 29188–29194.

Park, B.O., Ahrends, R., and Teruel, M.N. (2012). Consecutive Positive Feedback Loops Create a Bistable Switch that Controls Preadipocyte-to-Adipocyte Conversion. Cell Rep. *2*, 976–990.

Ran, F.A., Hsu, P.D., Lin, C.Y., Gootenberg, J.S., Konermann, S., Trevino, A.E., Scott, D.A., Inoue, A., Matoba, S., Zhang, Y., et al. (2013). Double nicking by RNA-guided CRISPR cas9 for enhanced genome editing specificity. Cell *154*, 1380–1389.

Shcherbo, D., Murphy, C.S., Ermakova, G. V, Solovieva, E. a, Chepurnykh, T. V, Shcheglov, A.S., Verkhusha, V. V, Pletnev, V.Z., Hazelwood, K.L., Roche, P.M., et al. (2009). Far-red fluorescent tags for protein imaging in living tissues. Biochem. J. *418*, 567–574.

Wolins, N.E., Quaynor, B.K., Skinner, J.R., Tzekov, A., Park, C., Choi, K., and Bickel, P.E. (2006). OP9 mouse stromal cells rapidly differentiate into adipocytes: characterization of a useful new model of adipogenesis. J. Lipid Res. *47*, 450–460.